Communication

Analysis of the E-region low-altitude quasi-periodic event in Low-latitudes of China

Lei Qiao , Gang Chen * , Mingkun Su , Chunxiao Yan , Erxiao Liu , Jun Wu

Posted Date: 3 October 2023

doi: 10.20944/preprints202310.0122.v1

Keywords: Low-latitude ionosphere; LQP echoes; Plasma instability

Communication

Analysis of the E-region Low-Altitude Quasi-Periodic Event in Low-Latitudes of China

Lei Qiao [1,2], Gang Chen [3,*], Mingkun Su [1], Chunxiao Yan [2], Erxiao Liu [1] and Jun Wu [1]

[1] Communication Engineering School, Hangzhou Dianzi University, Hangzhou 310018, China; qiaolei@hdu.edu.cn (L.Q.); mkshdu@hdu.edu.cn (M.S.); liuerxiao@hdu.edu.cn (E.L.); 42315@hdu.edu.cn (J.W.)

[2] State Key Laboratory of Space Weather, Chinese Academy of Sciences, Beijing 100190, China; qiaolei@hdu.edu.cn (L.Q.); cxyan@nssc.ac.cn (C.Y.)

[3] Electronic Information School, Wuhan University, Wuhan 430072, China; g.chen@whu.edu.cn (G.C.)

* Correspondence: g.chen@whu.edu.cn

Abstract: The low-altitude quasi-periodic (LQP) E-region echoes observed with the upgraded Hainan COherent scatter Phased Array Radar (HCOPAR) located in Hainan Island of China (19.5°N, 109.1°E) are presented. With the interferometry technique, the interferometry equations can be developed to investigate the structures of the irregularities. The results show that the plasma structures of the LQP echoes with negative slope mainly drifted southwestward almost horizontally, but they also drifted southeastward in some striations. According to the movement of the plasma structures, we find strong wind shear in the region where the LQP echoes were produced. Meanwhile, The periodicity of the LQP echoes may be related to the strength of the wind shear. It is proposed that the plasma structures are most likely produced by the Kelvin-Helmholtz instability (KHI).

Keywords: low-latitude ionosphere; LQP echoes; plasma instability

1. Introduction

Ionospheric E-region irregularities are the plasma structures arranged along magnetic field lines generated by the plasma instability process in the E-region. Due to the field-aligned property of the irregularities, the backscattered echoes of the E-region irregularities observed by the VHF radar often show some spacial patterns in the range-time-intensity (RTI) plot. It reflects the changes in the morphological and dynamic characteristics of the irregularities. The cause of quasi-periodic (QP) echoes has attracted a lot of attention. Yamamoto et al. first reported the QP echoes in mid-latitudes, which generally appeared after sunset with a period of 5-10 min and occurred at altitudes greater than 100 km [1]. Urbina et al. and Rao et al. first reported the QP echoes with altitudes below 100 km in the low and middle latitudes respectively [2-3]. They are named Low-altitude Quasi-period (LQP) echoes in order to distinguish them from typical QP echoes. Subsequently, LQP echoes have received attention from related scholars, and these echoes have been reported at both mid- and low- latitudes [4-10].

Fewer LQP echo events are observed in mid-latitudes, and the echo power is significantly lower than that of typical QP echoes above 100 km [3]. The more LQP events are observed at low-latitudes and the echo power is close to the typical QP echoes above 100 km, which suggests the LQP echoes are more beneficial to be generated at low-latitudes. In addition, case and statistical studies in the Gadanki area have shown that the daytime and nighttime occurrence rates of the LQP echoes are close, which is not consistent with the higher occurrence rate of typical QP echoes at night [9, 11]. The E-region continuous echoes [12], valley region irregularities [13, 14], and QP echoes [15-17] are also studied in the low latitude Hainan region of China. However, The corresponding studies of LQP echoes in low-latitudes of China are still relatively few.

In this paper, by using the interferometry technique with the upgraded Hainan COherent scatter Phased Array Radar (HCOPAR), we will observe the plasma patches drifting in the illuminating region, which is responsible for the LQP striations. In addition, the HCOPAR has a high range

Preprints (www.preprints.org) | NOT PEER-REVIEWED | Posted: 3 October 2023 doi:10.20944/preprints202310.0122.v1

resolution (~178 m) and a high temporal resolution (20 s). We hope to understand more clearly the characteristics of the LQP echoes with the help of the upgraded HCOPAR. The observation results of LQP echoes and the discussion are presented in Section 2. Conclusions are given in Section 3.

2. Observations and Discussion

The HCOPAR is located at Fuke, northwestern of Hainan Island of China (19.5°N, 109.1°E), which is marked with an triangle in Figure 1(a). The operating frequency of the radar is 47 MHz with the peak power of 54 kHz. As shown in array A in Figure 1(b), the initial antenna array of the HCOPAR consists of 72 linearly polarized Yagi antennas arranged in an 18×4 matrix. The Yagi antennas are mounted at an inclination of 62.5° to the ground, so that the beam is perpendicular to the magnetic field lines in the ionosphere. The half power beam width (HPBW) of the beam is 4.6° in azimuth direction and 21.7° in elevation direction [18]. After upgrading in 2020, array B and array C arranged in an 9×4 matrix were added, and the two arrays were only used to receive the echoes. The array A was used for transmission as well as reception, and the array B and C were employed only for reception. The space between the Yagi antenna elements is 0.7 wavelength. The phase center of array B is located 26.9 m northwest of array A, and the phase center of array C is located 40.2 m east of array B. With the interferometry technique, the angle of the meter-sclae irregularities can be measured in the illuminating region [19]. According to the layout of the antenna array, the interferometry equations for the HCOPAR can be developed to investigate the structures of the irregularities. It has been applied to study the daytime F-region irregularities with interferometry technique in low latitudes of China [20].

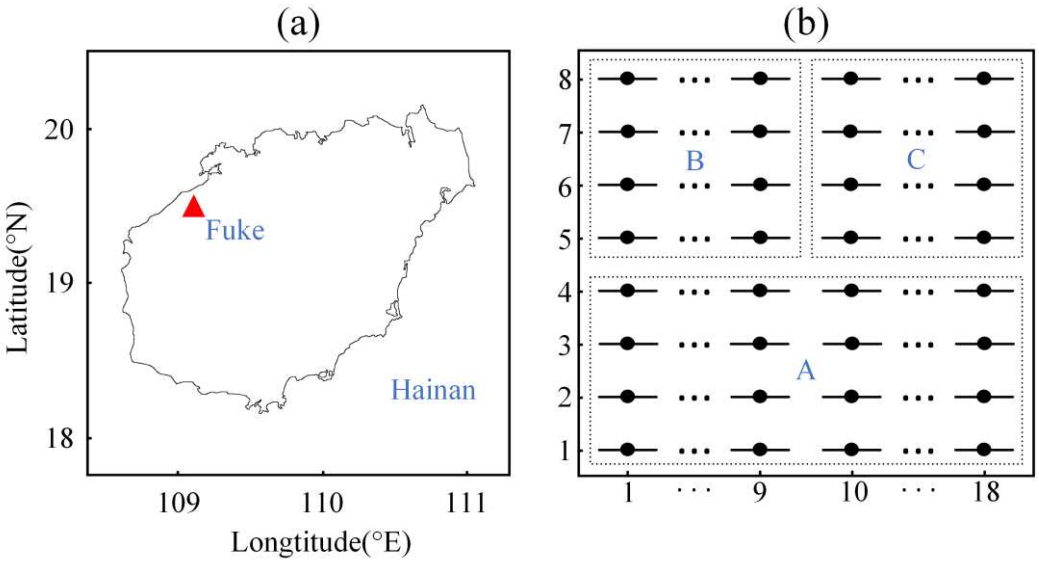

Figure 1. (a) The location and (b) the layout of the antenna array of the upgraded HCOPAR.

Figure 2(a) shows the height-time-intensity (HTI) plot of the observed echoes by the HCOPAR during 15:00-19:00 LT on March 12, 2020. Because of the high magnetic aspect angle sensitivity of field-aligned irregularities (FAI) [21], the height information is obtained by multiplying the distance by the cosine (cos 29.75°) of the magnetic inclination of the E-layer in this region. The radar was operated with 178 m range resolution and 10 s temporal resolution, and the fine variation of the FAIs at the spatial and temporal scales can be observed. As shown in Figure 2(a), there are two obvious LQP events. The first event is observed during 16:15-16:30 LT in the altitude range of 93.5-97 km, and the LQP structures has periods of about 64 s and mean SNR of 15 dB. The second event is observed during 18:00-18:50 LT in the altitude range of 91.5-95.5 km, and the LQP structures has periods of about 100 s and mean SNR of 13.6 dB.

Preprints (www.preprints.org) | NOT PEER-REVIEWED | Posted: 3 October 2023 doi:10.20944/preprints202310.0122.v1

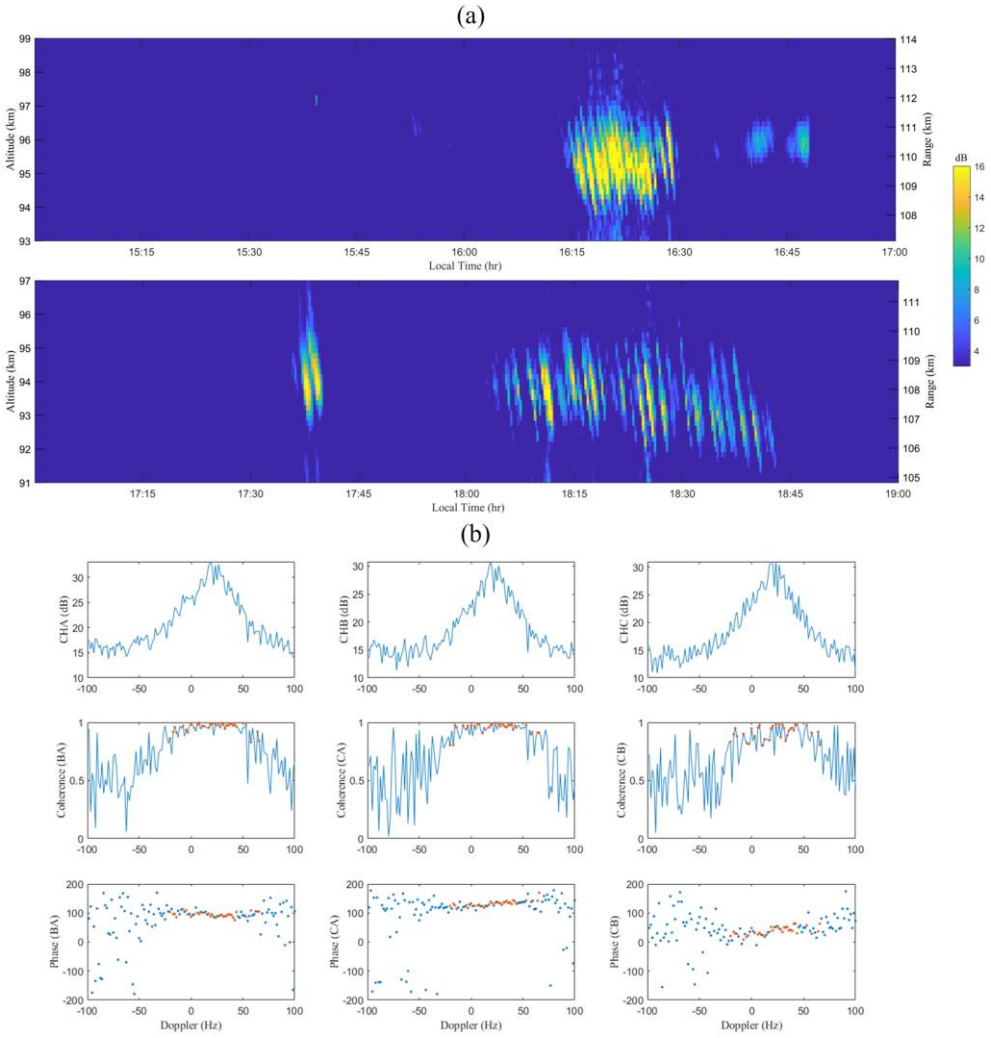

Figure 2. (a) The HTI plot of the observed echoes by the HCOPAR during 15:00-19:00 LT on March 12, 2020. (b) Examples of the Doppler spectra, coherence and phase of the echoes at the range of 110 km during 16:17:10-16:17:30 LT.

The pulse repetition frequency (PRF) of the radar is 200 Hz, and the non-coherent integration is 2. Thus, a group of 512 data points corresponds to data lengths of 5.12 s. The repetition period of the cycle is 20 s for data acquisition and signal processing. The 128 points of complex spectra were utilized to get the Doppler spectra for each channel. Before the spectrum analysis with the fast Fourier transform (FFT), the 512 complex data points within 20 s were divided into four parts. The Doppler spectra of each receiver is analyzed two by two for the correlation spectra, the four integrations were averaged to obtain the normalized correlation spectra. Taking the echoes at the range of 110 km during 16:17:10-16:17:30 LT as an example, Figure 2(b) shows the Doppler spectra and cross spectra for the three channels. The top panels show the Doppler spectra for each channel. The positive Doppler frequency denotes the target close to the radar. The middle and bottom panels show the coherence and phase of the same data. It can be found from Figure 2(b) that the phases are very close and concentrated around the spectral peak when the coherence is high, and phases with lower coherence have a random distribution. The spectral components with high coherence indicate the echoes from different channels come from the same scattering region. To ensure the quality of the echo reconstruction, the data with coherence greater than 0.8 and the phase difference of the three channels less than 3° are employed for the interferometry analysis, and the red points in the middle and bottom panels of Figure 2(b) meet the requirements.

To further understand the characteristics of LQP echoes, we discussed the overall spatial distribution of the irregularities. The phase spectrum of each data set is extracted, and the echo points

 doi:10.20944/preprints202310.0122.v1

that meet the above requirements are screened. After the phase correction, the points are projected on the mutually orthogonal planes to represent the echo regions. Figure 3(a) shows the echoes during 16:15-16:30 LT and 18:00-18:50 LT projected in the vertical plane by the vertical and north-south axes, where the solid lines on the left and right indicate the elevation angles of 61.35° and 59.05° respectively. The red and blue points represent the echoes during 16:15-16:30 LT and 18:00-18:50 LT respectively. The echo region during 16:15-16:30 LT has the scale of about 5 km in the north-south dimension and about 2 km in the vertical dimension, which looks like a parallelogram in space. It indicates that the irregularities move in the north-south direction regularly. The echo region during 18:00-18:50 UT has the scale of about 3 km in the vertical dimension, which is an irregular shape in space. The abnormal region is highlighted by black dashed lines, and it indicates that there are irregularities moving abnormally. Meanwhile, we find that the LQP structures are distributed in strips, which indicates the LQP structures are distributed along the magnetic lines. Figure 3(b) shows the projections of the echoes in the horizontal plane, where the solid lines on the left and right indicate the azimuth angle of -3.5° and 3.5° respectively. Different from the oblique stripes in Figure 3(a), the echoes are randomly distributed in the region with the scale of about 8 km in east-west dimension. Most of the echoes have the azimuth angles within 7°, which is larger than the half-power width of the main lobe (4.6°). Therefore, there are some echoes are received by the side lobe of the antenna. The echo regions during 16:15-16:30 LT and 18:00-18:50 LT are almost overlapping in the horizontal plane, which indites that the irregularities in the two time periods are generated in the same region. Figure 3(c) shows the echoes projected in the vertical plane by the vertical and east-west axes. The echoes regions during during 16:15-16:30 LT and 18:00-18:50 LT have almost the same scales in the north-south dimension and vertical dimension, except the abnormal region highlighted by black dashed lines in the height range of 91.8-93 km. The height is the same as that of the abnormal region in Figure 3(a), and we will discuss the anomaly region further.

Preprints (www.preprints.org) | NOT PEER-REVIEWED | Posted: 3 October 2023 doi:10.20944/preprints202310.0122.v1

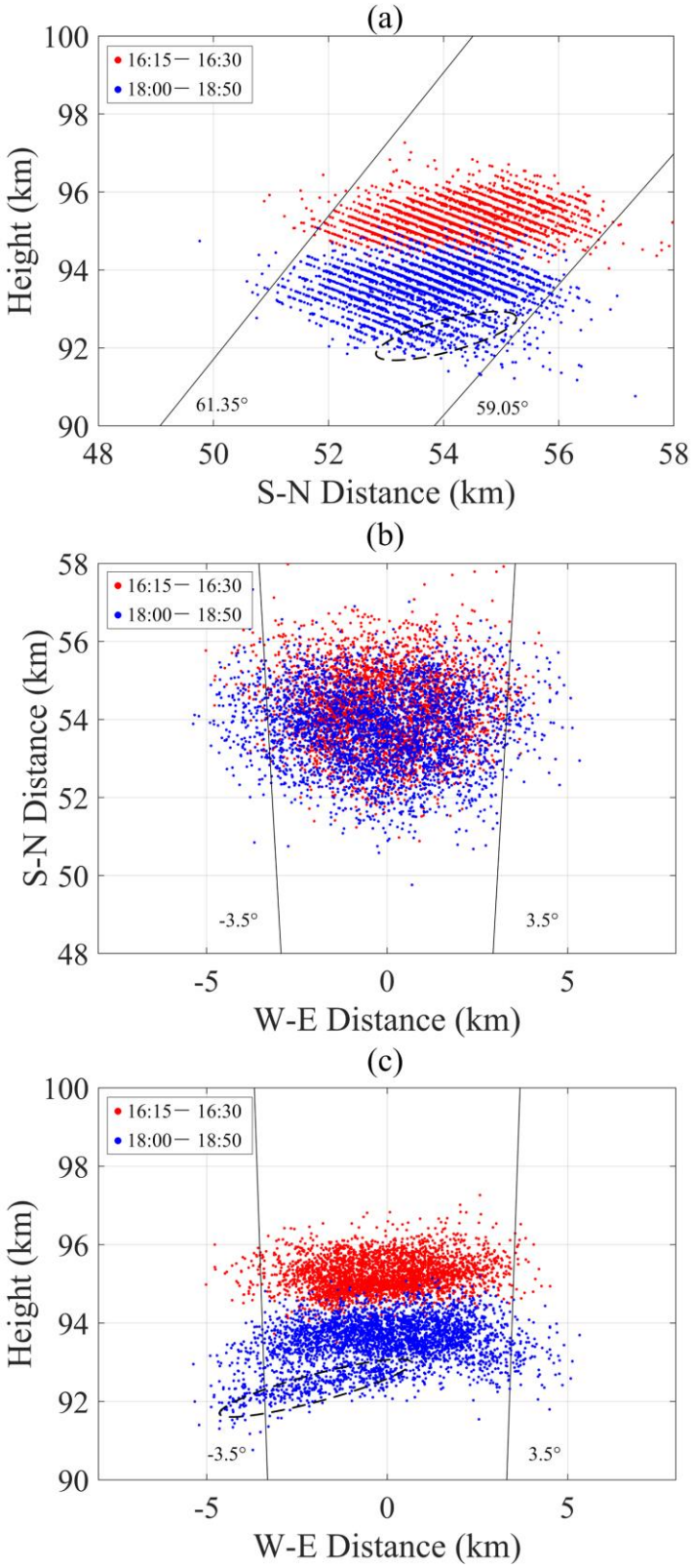

Figure 3. (a) The echoes during 16:15-16:30 LT and 18:00-18:50 LT projected in the vertical plane by the vertical and north-south axes. (b) The echoes projected in the horizontal plane by the north-south and east-west axes. (c) The echoes projected in the vertical plane by the vertical and east-west axes.

Figure 4(a) shows the LQP echoes observed during 16:15-16:30 LT. There are 14 significant LQP striations, with a height extension of 1 to 2 km, and a period of about 64 s. The event lasted about 15

Preprints (www.preprints.org) | NOT PEER-REVIEWED | Posted: 3 October 2023 doi:10.20944/preprints202310.0122.v1

minutes, and all the striations had a negative slope. During the SEEK-2 campaign, the comparison of echoes obtained by the LTPR and the FAR revealed that echoing regions drifted with a southward velocity component, and the interferometry observation of the LTPR revealed that the negative range rate of the QP striations corresponded to an westward velocity component for the moving echoing regions [22]. Urbina et al. showed the backscattering regions drifted in the westward direction [7], but Pan et al. found a northwest to southeast drifting motion dominates within a preferential area [8]. To confirm what is happened for the LQP structures, we tracked the positions of the LQP striations. The spatial structure of the LQP striations are reconstructed depending on the angular positions of the FAIs in the echoing region. To distinguish the state of each striation, we selected different colors to represent the spatial distributions of the irregularities at different times, and the arrows indicate the drifting direction of the LQP structures. Figure 4(b) shows the continuous changes of the spatial distributions for typical traces 1, 2 and 3 on the orthogonal planes. The plasma structures in traces 1, 2 and 3 moved southward at the trace velocity of about 44.0, 41.6, and 51.5 m/s respectively. The plasma structures in traces 1, 2 and 3 moved downward at the trace velocity of about 8.3, 11.0, and 10.9 m/s respectively, so they moved at an almost constant altitude. The plasma structures in traces 1, 2 and 3 moved westward at the trace velocity of about 26.8, 38.0, and 62.3 m/s respectively. Therefore, the LQP structures in the three traces drifted southwestward almost horizontally. Due to the high aspect sensitivity, the plasma structures can only be observed in the elevation range of 59.05°-61.35°, so the plasma structures drifted into and out of the radar volume to form the LQP striations in the HTI plot.

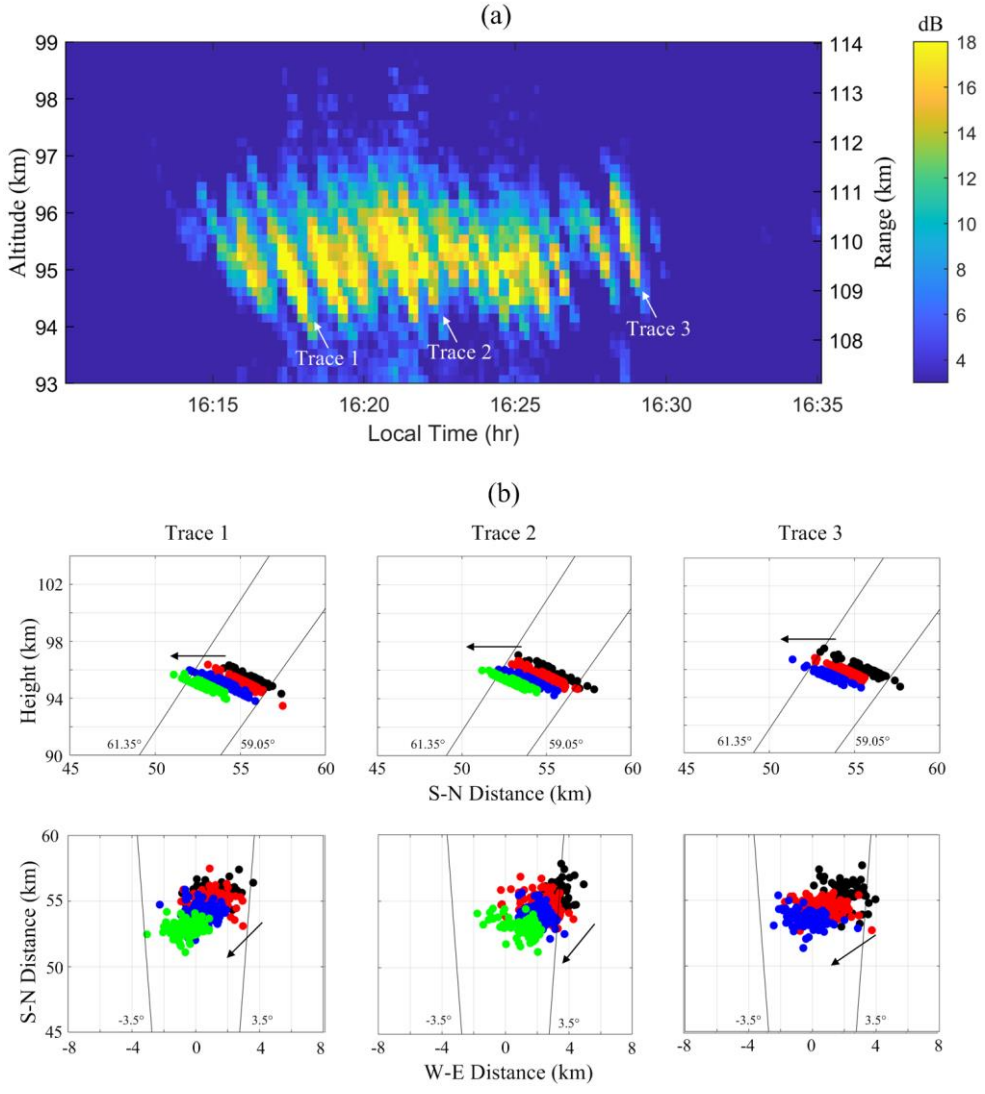

Preprints (www.preprints.org) | NOT PEER-REVIEWED | Posted: 3 October 2023 doi:10.20944/preprints202310.0122.v1

Figure 4. (a) The LQP echoes observed during 16:15-16:30 LT. (b) The continuous changes of the spatial distributions for traces 1, 2 and 3 on the orthogonal planes.

Figure 5(a) shows the LQP echoes observed during 18:00-18:50 LT. There are 25 significant LQP striations, with a height extension of 1 to 3 km, and a period of about 96 s. The event lasted about 40 minutes, and all the striations had a negative slope. Figure 5(b) shows the continuous changes of the spatial distributions for typical traces 4, 5 and 6 on the orthogonal planes. The plasma structures in traces 4, 5 and 6 moved southward at the trace velocity of about 45.1, 53.9, and 50.1 m/s respectively. The meridional velocity is close to the observation during 16:15-16:30 LT, which indicates the meridional wind was almost constant. As shown in Figure 5(b), The plasma structures in trace 4 drifted westward at the trace velocity of about 60.0 m/s, which is similar to traces 1, 2 and 3. However, the plasma structures in trace 5 and 6 drifted eastward at the trace velocity of about 0.3 and 15.4 m/s respectively. Therefore, the latitudinal motion of the plasma structures in the striations during 18:00-18:50 LT is more complex. According to what has been discussed above, the plasma structures in the striations with negative slope mainly drifted southwestward, but they also drifted southeastward in some striations. It indicates that there was less variation in meridional winds, and more variation in latitudinal winds. Therefore, the abnormal region in Figure 3 was mainly induced by the eastward plasma structures.

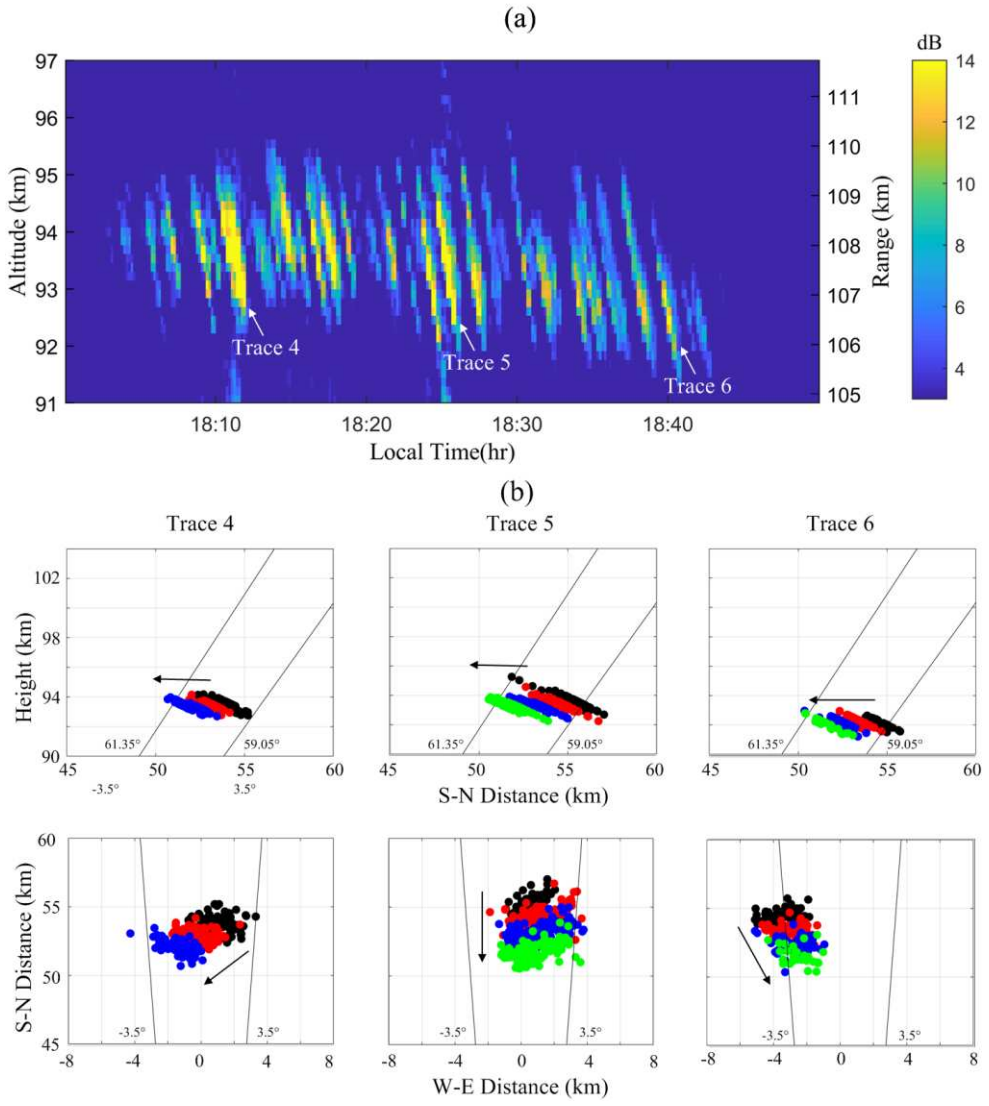

Figure 5. (a) The LQP echoes observed during 18:00-18:50 LT. (b) The continuous changes of the spatial distributions for traces 4, 5 and 6 on the orthogonal planes.

Preprints (www.preprints.org) | NOT PEER-REVIEWED | Posted: 3 October 2023 doi:10.20944/preprints202310.0122.v1

According to the changes of the spatial distributions for each striation, the mean projection velocities in the latitudinal, and meridional directions of different striations can be calculated. Figure 6(a) shows the results during 16:15-16:30 LT, and Figure 6(b) shows the results during 18:05-18:40 LT. The red, and blue dots and lines indicate latitudinal, and longitudinal velocities respectively, and the lines are the results of fitting the points. It should be note that some striations with low SNR were deleted. The mean latitudinal velocities of the striations during 16:15-16:30 LT and 18:05-18:40 LT were 45.3 m/s and 46.6 m/s, and the mean latitudinal velocities were 31.0 m/s and 13.3 m/s. The meridional velocities were closer in the two time periods, while the differences in latitudinal velocities were larger. The similarity in the morphology of the LQP echoes in these two time periods was the negative slope, while the difference was the periodicity. Therefore, the southward wind might induce the negative slope. It is consistent with the statistical analysis of Chen et al. [16]. The latitudinal wind might be an important cause of the different periodicity in these two time periods.

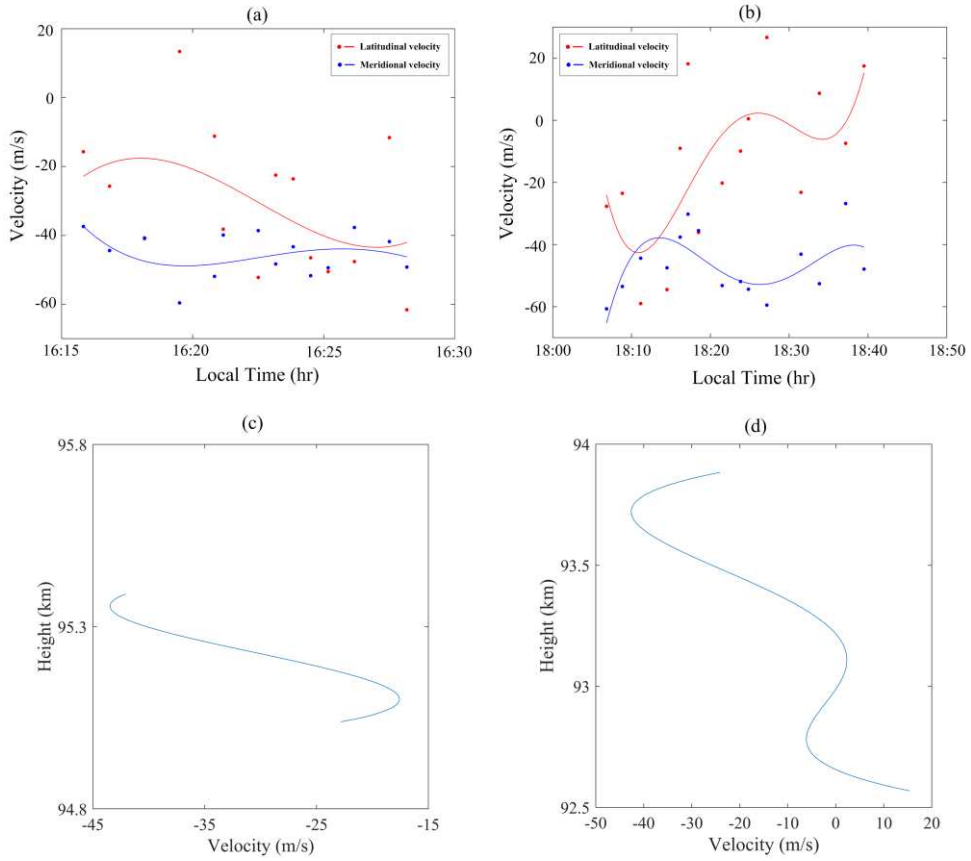

Figure 6. The mean projection velocities in the latitudinal and meridional directions of the striations during (a) 16:15-16:30 LT and (b) 18:05-18:40 LT. The height variations of the plasma structures' latitudinal velocities during (c) 16:15-16:30 LT and (d) 18:05-18:40 LT.

In order to gain a deeper understanding of the LQP echoes generation mechanism, we further analyzed the data. Figure 6(c) and Figure 6(d) displays the height variations of the plasma structures' latitudinal velocities during 16:15-16:30 LT and 18:05-18:40 LT. The trace velocity of the patch reflects the the background wind velocity in the collision dominated lower E-region (<100 km). As shown in Figure 6(c) and Figure 6(d), there are significant shears in the latitudinal velocities of the plasma structures. The shear during 16:15-16:30 LT was 101 (m/s)/km , and the shear during 18:05-18:40 LT was 50 (m/s)/km. The results indicate that there were the neutral wind shears in the region where the LQP echoes were produced, and the wind shear during 16:15-16:30 LT was larger than that during 18:05-18:40 LT. In previous studies, researchers have generally assumed that the neutral wind shear driven Kelvin-Helmholtz instability (KHI) accounts for the LQP echoes [10]. The result is consistent with the assumption. The long-lived metallic ions from meteor ablation and deposition are converged by the wind shear to from the thin layer under the effect of the Earth's magnetic field [23]. When the

Richardson number Ri is <0.25, the thin layer becomes unstable for KHI [24]. The KH billows associated with the instability produce the horizontal plasma density structures [5]. The plasma density structures embedded in the background wind can produce the QP striations, when they drift into and out of the radar volume. Pan et al. reported that the striation periodicity of the QP echoes was related to mean velocity in the unstable shear layer, i.e., the range rate velocity [25]. We found the velocity shear during 16:15-16:30 LT was twice that during 18:05-18:40 LT, while the striation periodicity during 16:15-16:30 LT was half that during during 18:05-18:40 LT. It means that the striation periodicity is inversely related to the wind shear. Therefore, the periodicity of the striations is more likely related to the strength of the wind shear.

3. Conclusions

We have presented the high resolution measurements of the LQP echoes with the upgraded HCOPAR. The LQP echoes with a negative slope is mainly induced by the southward drifting plasma structures. The periodicity of the LQP echoes is more likely related to the strength of the wind shear. The KHI may produce the horizontal plasma density structures resulting in the LQP echoes.

Author Contributions: Conceptualization, L.Q. and G.C.; methodology L.Q.; investigation, L.Q.; validation, M.S.; formal analysis, C.Y.; resources, C.Y.; visualization, E.L.; funding acquisition, L.Q. and G.C. All authors have read and agreed to the published version of the manuscript reported.

Funding: This project was supported by the National Natural Science Foundation of China (42274197), the Fundamental Research Funds for the Central Universities (2042023kf0200), the Specialized Research Fund for State Key Laboratories, and the Natural Science Foundation of Zhejiang Province under grant LQ22D040001.

Data Availability Statement: The HCOPAR data are obtained from the Chinese Meridian Project website: https://data.meridianproject.ac.cn

Acknowledgments: We appreciate the editors and the anonymous reviewers for their insightful comments and suggestions to improve this paper.

Conflicts of Interest: The authors declare no conflict of interest.

References

1. Yamamoto, M.; Fukao, S.; Woodman, R. F.; et al. Mid-latitude E region field-aligned irregularities observed with the MU radar. *Journal of Geophysical Research: Space Physics*, **1991**, 96(A9), 15943-15949.
2. Urbina, J.; Kudeki, E.; Franke, S. J.; et al. 50 MHz radar observations of mid-latitude E-region irregularities at Camp Santiago, Puerto Rico. *Geophys. Res. Lett.*, **2000**, 27(18), 2853-2856.
3. Rao, P. B.; Yamamoto, M.; Uchida, A.; et al. MU radar observations of kilometer-scale waves in the mid latitude lower E-region. *Geophys. Res. Lett.*, **2000**, 27(22), 3667-3670.
4. Patra, A. K.; Sripathi, S.; Siva, K. V.; et al. Evidence of kilometer-scale waves in the lower E region from high resolution VHF radar observations over Gadanki. *Geophys. Res. Lett.*, **2002**, 29(10), 1371-1374.
5. Pan, C. J.; Rao, P. B. Low altitude quasi-periodic radar echoes observed by the Gadanki VHF radar. *Geophys. Res. Lett.*, **2002**, 29(11), 251-254.
6. Sripathi, S.; Patra, A. K.; Sivakumar, V.; et al. 2003. Shear instability as a source of the daytime quasi-periodic radar echoes observed by the Gadanki VHF radar. *Geophys. Res. Lett.*, **2003**, 30(22), 2149.
7. Urbina, J.; Kudeki, E.; Franke, S. J.; et al. 2004. Analysis of a mid-latitude E-region LQP event observed during the Coqui 2 Campaign. *Geophys. Res. Lett.*, **2004**, 31(14), 805.
8. Pan, C. J.; Röttger, J.; Chen, C. L. Radar investigations of low-altitude quasi-periodic echoes in Chung-Li. *Geophys. Res. Lett.*, **2005**, 32(11), 102.
9. Patra, A. K.; Sripathi, S.; Rao, P. B.; et al. Gadanki radar observations of daytime E region echoes and structures extending down to 87 km. *Ann. Geophys.*, **2006**, 24(7), 1861-1869.
10. Patra, A. K., Rao, N. V., Choudhary, R. K. Daytime low-altitude quasi-periodic echoes at Gadanki: Understanding of their generation mechanism in the light of their Doppler characteristics. *Geophys. Res. Lett.*, **2008**, 36(5).
11. Venkateswara, N. V.; Patra, A. K.; et al. Morphology and seasonal characteristics of low latitude E-region quasiperiodic echoes studied using large database of Gadanki radar observations. *Journal of Geophysical Research: Space Physics*, **2008**, 13, A07312.
12. Ning, B.; Li, G.; Hu, L.; et al. Observations on the field-aligned irregularities using Sanya VHF radar: 1. Ionospheric E-region continuous echoes (in Chinese). *Chin. J. Geophys.*, **2013**, 56, 719–730.

13. Li, G.; Ning, B.; Patra, A. K.; et al. Investigation of low-latitude E and valley region irregularities: Their relationship to equatorial plasma bubble bifurcation. *Journal of Geophysical Research: Space Physics*, **2011**, 116(11), 11319.
14. Li, G.; Ning, B.; Patra, A. K.; et al. On the linkage of daytime 150 km echoes and abnormal intermediate layer traces over Sany. *Journal of Geophysical Research: Space Physics*, **2013**, 118(11), 7262-7267.
15. Li, G.; Ning B, Hu L, et al. Observations on the field-aligned irregularities using Sanya VHF radar: 2. Low latitude Ionospheric E-region quasi-periodic echoes in the East Asian sector (in Chinese). *Chin. J. Geophys.*, **2013**, 56, 2141-2151.
16. Chen, G.; Jin, H.; Huang, X.; et al. Strong correlation between quasiperiodic echoes and plasma drift in the E region. *Journal of Geophysical Research: Space Physics*, **2015**, 120(10), 9110-9116.
17. Xie, H.; Li, G.; Zhao, X.; et al. Coupling Between E Region Quasi-Periodic Echoes and F Region Medium-Scale Traveling Ionospheric Disturbances at Low Latitudes. *Journal of Geophysical Research: Space Physics*, **2020**, 125(5), A027720.
18. Chen, G.; Jin, H,; Yan, J.; Cui, X.; Zhang, S.; Yan, C.; et al. Hainan coherent scatter phased array radar (HCOPAR): System design and ionospheric irregularity observations. *IEEE Transactions on Geoscience and Remote Sensing*, **2017**, 55(8), 4757-4765.
19. Wang, C. Y.; Chu, Y. H.; Su, C. L.; et al. Statistical investigations of layer-type and clump-type plasma structures of 3-m field-aligned irregularities in nighttime sporadic e region made with chung-li vhf radar. *Journal of Geophysical Research: Space Physics*, **2011**, 116, A12311.
20. He, Z.; Chen, G.; Yan, C.; et al. Imaging Radar Observations of the Daytime F-Region Irregularities in Low-Latitudes of China. *Journal of Geophysical Research: Space Physics*. **2023**, 128(2).
21. Riggin, D.; Swartz, W. E.; Providakes, J.; et al. Radar studies of long wavelength waves associated with mid latitude sporadic E layers. *Journal of Geophysical Research*, **1986**, 91(A7), 8011-8024.
22. Saito, S.; Yamamoto, M.; Fukao, S.; et al. Radar observations of field-aligned plasma irregularities in the seek-2 campaign. *Annales Geophysicae*, **2005**, 23(7), 2307-2318.
23. Mathews, J. D. Sporadic-E: Current views and recent progress. *Journal of Atmospheric and Solar-Terrestrial Physics*, **1998**, 60(4), 413-435.
24. Larsen, M. F. A shear instability seeding mechanism for quasi-periodic radar echoes, *J. Geophys. Res.*, **2000**, 105(24) 931-940.
25. Pan, C. J. and Larsen, M. F. (2000). Observations of qp radar echo structure consistent with neutral wind shear control of the initiation mechanism. *Geophys. Res. Lett.*, **2000**, 27(6), 867–870.